

Photochemistry of atomic oxygen green and red-doublet emissions in comets at larger heliocentric distances

Susarla Raghuram* and Anil Bhardwaj

Space Physics Laboratory, Vikram Sarabhai Space Center, Trivandrum 695022, India

Accepted for publication

ABSTRACT

Context. In comets the atomic oxygen green (5577 Å) to red-doublet (6300, 6364 Å) emission intensity ratio (G/R ratio) of 0.1 has been used to confirm H₂O as the parent species producing forbidden oxygen emission lines. The larger (>0.1) value of G/R ratio observed in a few comets is ascribed to the presence of higher CO₂ and CO relative abundances in the cometary coma.

Aims. We aim to study the effect of CO₂ and CO relative abundances on the observed G/R ratio in comets observed at large (>2 au) heliocentric distances by accounting for important production and loss processes of O(¹S) and O(¹D) atoms in the cometary coma.

Methods. Recently we have developed a coupled chemistry-emission model to study photochemistry of O(¹S) and O(¹D) atoms and the production of green and red-doublet emissions in comets Hyakutake and Hale-Bopp. In the present work we applied the model to six comets where green and red-doublet emissions are observed when they are beyond 2 au from the Sun.

Results. The collisional quenching of O(¹S) and O(¹D) can alter the G/R ratio more significantly than that due to change in the relative abundances of CO₂ and CO. In a water-dominated cometary coma and with significant (>10%) CO₂ relative abundance, photodissociation of H₂O mainly governs the red-doublet emission, whereas CO₂ controls the green line emission. If a comet has equal composition of CO₂ and H₂O, then ~50% of red-doublet emission intensity is controlled by the photodissociation of CO₂. The role of CO photodissociation is insignificant in producing both green and red-doublet emission lines and consequently in determining the G/R ratio. Involvement of multiple production sources in the O(¹S) formation may be the reason for the observed higher green line width than that of red lines. The G/R ratio values and green and red-doublet line widths calculated by the model are consistent with the observation.

Conclusions. Our model calculations suggest that in low gas production rate comets the G/R ratio greater than 0.1 can be used to constrain the upper limit of CO₂ relative abundance provided the slit-projected area on the coma is larger than the collisional zone. If a comet has equal abundances of CO₂ and H₂O, then the red-doublet emission is significantly (~50%) controlled by CO₂ photodissociation and thus the G/R ratio is not suitable for estimating CO₂ relative abundance.

Key words. Atomic processes – Molecular processes – Comets: general – Comets: C/2006 W3 (Christensen): C/2007 Q3 (Siding Spring): C/2003 K4 (LINEAR): 116P/Wild 4: C/2009 P1 (Garradd): C/2001 Q4 (NEAT) – Line: profiles – Line: formation

1. Introduction

Green (5577 Å) and red-doublet (6300, 6364 Å) emissions are due to the electronic transition of oxygen atoms from metastable ¹S and ¹D states, respectively, to the ground ³P state. Since O(¹S) and O(¹D) are metastable states, resonance fluorescence by solar photons is not an effective excitation mechanism for populating these states. Dissociative excitation of O-bearing neutrals by photons and photoelectrons, and thermal recombination of atomic oxygen constituted ions are the sources of these metastable states in the cometary coma (Bhardwaj & Haider 2002; Bhardwaj & Raghuram 2012; Raghuram & Bhardwaj 2013). Most of the comets observed around heliocentric distance of 1 au have H₂O as the principal constituent in the cometary coma (Bockelée-Morvan et al. 2004). Based on the theoretical work of Festou & Feldman (1981) green to red-doublet emission intensity ratio (hereafter G/R ratio) of 0.1 has customarily been used as a benchmark to confirm the parent source of these prompt emissions as H₂O in several comets observed around 1 au from the Sun (Cochran 1984, 2008; Morrison et al. 1997; Zhang et al. 2001; Cochran & Cochran 2001; Furusho et al. 2006; Capria et al.

2005, 2008, 2010). The observed G/R ratio of more than 0.1 has been attributed to higher relative abundances of CO₂ and CO (Furusho et al. 2006; Capria et al. 2010; McKay et al. 2012; Decock et al. 2013). Since no experimental cross section or yield for the production of O(¹S) from H₂O is available in the literature, the calculated photorates of Festou & Feldman (1981) have been questioned by Huestis & Slanger (2006). In a H₂O-dominated cometary coma, the red-doublet emission intensity is determined by formation and destruction rates of O(¹D) (Bhardwaj & Haider 2002; Bhardwaj & Raghuram 2012; Raghuram & Bhardwaj 2013). Since the red-doublet emission is mainly governed by photodissociation of H₂O, the observed intensity of 6300 Å has been used to estimate the production rate as well as to understand the spatial distribution of H₂O in the cometary coma (e.g. Delsemme & Combi 1976; Delsemme & Combi 1979; Fink & Johnson 1984; Schultz et al. 1992; Morgenthaler et al. 2001; Furusho et al. 2006).

We have recently developed a coupled chemistry-emission model for the production of green and red-doublet emissions by accounting for important production and loss mechanisms of O(¹S) and O(¹D) atoms. The model has been applied to comets Hyakutake (Bhardwaj & Raghuram 2012) and Hale-Bopp (Raghuram & Bhardwaj 2013). Our model calculations

* Corresponding author : raghuramsusarla@gmail.com

showed that in a H_2O -dominated cometary coma more than 90% of the $\text{O}(\text{}^1\text{D})$ is populated via photodissociative excitation of H_2O and the rest through photodissociation of CO_2 and CO . We also demonstrated that the G/R ratio depends not only on the photochemistry involved in the formation of $\text{O}(\text{}^1\text{D})$ and $\text{O}(\text{}^1\text{S})$, but also on the projected area observed on the comet, which is a function of slit dimension and geocentric distance of the comet (Bhardwaj & Raghuram 2012). The model calculations on comets Hyakutake and Hale-Bopp showed that the intensity of the [OI] 6300 Å line is largely governed by photodissociation of H_2O , whereas the [OI] 5577 Å emission line is mainly controlled by the photodissociation of both H_2O and CO_2 . It is also suggested that CO_2 can produce $\text{O}(\text{}^1\text{S})$ more efficiently than H_2O . The calculated mean excess energy profiles in various photodissociation processes showed that the photodissociation of CO_2 can produce $\text{O}(\text{}^1\text{S})$ with higher excess velocity compared to the photodissociation of H_2O (Raghuram & Bhardwaj 2013). All these calculations are carried out at ~ 1 au.

At larger heliocentric distances the cometary coma is composed of larger proportions of CO and CO_2 than at 1 au (Meech & Svoreň 2004; Crovisier et al. 1999; Biver et al. 1997, 1999; Bockelée-Morvan et al. 2004, 2010). At heliocentric distances of more than 2 au the prompt emissions of atomic oxygen are observed in several comets, viz. C/2007 Q3 (Siding Spring), C/2006 W3 (Christensen), C/2009 P1 (Garradd), C/2001 Q4 (NEAT), 116P/Wild 4, and C/2003 K4 (LINEAR) (Furusho et al. 2006; McKay et al. 2012; Decock et al. 2013). Assuming that CO_2 and CO are the main sources of green and red-doublet emissions, the observed G/R ratio in comets at large heliocentric distances (> 2 au) has been used to estimate the CO_2 abundance in comets (Decock et al. 2013; McKay et al. 2012).

The present study is aimed at studying the photochemistry of $\text{O}(\text{}^1\text{S})$ and $\text{O}(\text{}^1\text{D})$ atoms and associated green and red-doublet emission production mechanisms in the above mentioned six comets at larger heliocentric distance (> 2 au) where the gas production rate of CO can be equal to that of H_2O . One of the objectives of the study is to verify whether the G/R ratio value can be used to infer the CO_2 relative abundance, with respect to H_2O , in the comets that are observed at larger heliocentric distances. In this study we have shown that even at large heliocentric distances, the photodissociation of CO is only a minor source of $\text{O}(\text{}^1\text{S})$ and $\text{O}(\text{}^1\text{D})$ atoms, and its impact on the G/R ratio is negligible. The red-doublet emission intensity is mainly governed by H_2O , while the green line emission intensity is controlled by CO_2 . We have also demonstrated that collisional quenching can significantly change the observed G/R ratio and that its impact on the G/R ratio is much greater than that due to variation in the CO_2 and H_2O abundances.

2. Model

The details of model and the photochemical reactions considered in the model are presented in our previous works (Bhardwaj & Raghuram 2012; Raghuram & Bhardwaj 2013). Here we present the input parameters that have been used in the model for the calculation of green and red-doublet emission intensities for the observed conditions of six comets (viz. 116P/Wild 4, C/2003 K4 (LINEAR), C/2007 Q3 (Siding Spring), C/2006 W3 (Christensen), C/2009 P1 (Garradd), C/2001 Q4 (NEAT)). The photochemical reaction network and cross sections of photon and electron impact processes that have been considered in our previous work remain the same for the present calculation. The photoelectron impact excitation reactions are accounted for by degrading solar extreme ultraviolet

(EUV) generated photoelectrons and electron impact cross sections in the cometary coma using the analytical yield spectrum (AYS) technique which is based on the Monte Carlo method. Details of the AYS approach and the method for calculating photoelectron flux and excitation rates are given in our earlier papers and references therein (Bhardwaj 1999; Haider & Bhardwaj 2005; Bhardwaj & Raghuram 2011; Raghuram & Bhardwaj 2012; Bhardwaj & Raghuram 2012). The production and loss mechanisms for the $\text{O}(\text{}^1\text{S})$ and $\text{O}(\text{}^1\text{D})$ considered in the model calculations are presented in our previous papers (Bhardwaj & Raghuram 2012; Raghuram & Bhardwaj 2013). Only the dominant O-bearing neutral species H_2O , CO_2 , and CO are considered in the present model.

The neutral gas production rates used in the model calculations for different comets during observation periods of oxygen emission lines are tabulated in Table 1. In some comets these gas production rates are not measured, and so we have made a reasonable approximation to incorporate CO_2 and CO in the model. However, we vary the CO_2 and CO relative abundances on these comets to assess the impact on the green and red-doublet emission intensities and subsequently on the G/R ratio.

Furusho et al. (2006) observed the forbidden oxygen lines in comet 116P/Wild 4 when it was at 2.4 au from the Sun. Using the infrared satellite AKARI, Ootsubo et al. (2012) measured the H_2O production rate in this comet as $\sim 1 \times 10^{27} \text{ s}^{-1}$ and abundance of CO_2 was found to be 10% relative to the water at heliocentric distance of 2.22 au. Ootsubo et al. (2012) also determined the upper limit for CO abundance in this comet as 20% relative to water. In our model we have used these measured gas production rates and relative abundances as input assuming that these values did not vary significantly in this comet from 2.2 au to 2.4 au.

Using the SPITZER space telescope, Woodward et al. (2007) measured the H_2O production rate in comet C/2003 K4 (LINEAR) as $2.43 \times 10^{29} \text{ s}^{-1}$ when the comet was at 1.76 au from the Sun during pre-perihelion. Decock et al. (2013) observed atomic oxygen forbidden lines in this comet when it was at 2.6 au heliocentric distance. Since the H_2O production rate was not measured at 2.6 au we scaled the Woodward et al. (2007) measured H_2O production rate to heliocentric distance of 2.6 au assuming that it varies as the inverse square of heliocentric distance. However, we evaluate the impact of the estimated H_2O production rate on the calculated G/R by decreasing its value by a factor of 2. Since CO_2 and CO are not observed in this comet we have assumed their abundances to be 10% and 25% relative to H_2O , respectively. We show that CO does not play a significant role in determining green and red-doublet emission line intensities, whereas the CO_2 abundance is important in determining the G/R ratio.

In comet C/2007 Q3 (Siding Spring), only the [OI] 6300 Å emission line was observed and the intensity of [OI] 5577 Å was estimated with a 3σ upper limit when it was at a heliocentric distance of 2.96 au (McKay et al. 2012). The AKARI satellite detected both H_2O and CO_2 in comet C/2007 Q3 during its pre-perihelion period and measured the CO_2 relative abundance as 17% relative to H_2O production rate when the comet was at a heliocentric distance of 3.3 au (Ootsubo et al. 2012). Assuming that the photodissociation of H_2O is the major source for the observed [OI] 6300 Å emission, McKay et al. (2012) inferred the H_2O production rate in comet C/2007 Q3 as $1.8 \times 10^{27} \text{ s}^{-1}$ which is smaller by a factor of 2 than the Ootsubo et al. (2012) measurement. Ootsubo et al. (2012) observation covers a larger ($43'' \times 43''$) projected area on the coma which can account for most

Table 1. Observational conditions (slit dimension, heliocentric (r), and geocentric (Δ) distances) of various comets, corresponding H₂O production rates and CO₂ and CO relative abundances relative to H₂O, and comparison of calculated green to red-doublet emission intensity ratios (G/R ratio) with the observations.

Comet	r (au)	Δ (au)	Slit dimension (" × ")	Q(H ₂ O) (s ⁻¹)	CO ₂ [†] (%)	CO [†] (%)	G/R ratio cal. obs.	Reference [‡]
116P/Wild 4	2.40	1.4	8 × 1	1 × 10 ^{27*}	10	20	0.09 0.15	Furusho et al. (2006)
C/2003 K4 (LINEAR)	2.60	2.36	0.80 × 11	1 × 10 ^{29†}	10 [‡]	25 [‡]	0.09 0.09	Decock et al. (2013)
C/2007 Q3 (Siding Spring)	2.96	2.48	3.20 × 1.6	4 × 10 ^{27*}	17	10	0.12 0.20	McKay et al. (2012)
C/2006 W3 (Christensen)	3.13	2.35	3.20 × 1.6	2.0 × 10 ^{28*}	42	98	0.18 0.24 ± 0.08	McKay et al. (2012)
C/2009 P1 (Garradd)	3.25	3.50	0.44 × 12	2.3 × 10 ^{27***}	25 [‡]	100 [‡]	0.14 0.21	Decock et al. (2013)
C/2001 Q4 (NEAT)	3.70	3.40	0.45 × 11	3.8 × 10 ^{27**}	75 [‡]	100 [‡]	0.23 0.33	Decock et al. (2013)
comet X [§]	3.70	3.40	0.45 × 11	4 × 10 ²⁷	100	100	0.25 –	–

*Ootsubo et al. (2012); **Combi et al. (2009); ***Bodewits et al. (2012); [‡]Assumed; [†]See text; [§]comet X is a hypothetical comet similar to the observational condition of comet NEAT, but having equal gas production rate of H₂O, CO₂, and CO; cal. = Calculated, obs. = Observation. [‡]Reference is for the observed G/R ratio value on the corresponding comet.

of the H₂O produced from extended distributed sources like icy grains in the coma in the observed field of view compared to that of the McKay et al. (2012) observation (3.2'' × 1.62''). Hence, we have used the Ootsubo et al. (2012) measured gas production rates in the model. We have taken the H₂O production rate on comet C/2007 Q3 as 4 × 10²⁷ s⁻¹ with 17% and 10% relative abundances of CO₂ and CO with respect to water, respectively, in our model.

By making radio observations on comet C/2006 W3 (Christensen), Bockelée-Morvan et al. (2010) derived H₂O and CO production rates as 4.2 × 10²⁸ and 3.9 × 10²⁸ s⁻¹, respectively. During this measurement the comet was at a heliocentric distance of 3.2 au. These values are higher by a factor of 2 compared to the infrared satellite observed values reported by Ootsubo et al. (2012) which were derived when the comet was nearly at the same heliocentric distance. Ootsubo et al. (2012) reported 42% and 98% of CO₂ and CO abundances relative to H₂O, respectively, in this comet when it was at 3.13 au. During the green and red-doublet emission observation, comet C/2006 W3 was at a heliocentric distance of 3.13 au (McKay et al. 2012). For this comet we have used the Ootsubo et al. (2012) measured H₂O production rate as well as CO₂ and CO relative abundances in our model.

The H₂O production rate in comet C/2009 P1 (Garradd) beyond 2 au has been reported by various workers (Paganini et al. 2012; Villanueva et al. 2012; Bodewits et al. 2012; Combi et al. 2013; Farnham et al. 2012; Feaga et al. 2012). Using the SWIFT satellite, Bodewits et al. (2012) observed the OH 3080 Å emission line in comet C/2009 P1 and derived the H₂O production rate when it was between 2 au and 4 au heliocentric distances. We have taken H₂O production at 3.25 au from the Sun as 2.3 × 10²⁷ s⁻¹ by linearly interpolating the Bodewits et al. (2012) derived production rates between 3 au and 3.5 au heliocentric distances. Decock et al. (2013) used the observed G/R ratio at 3.25 au and estimated that around 25% CO₂ abundance relative to H₂O was present in this comet. We assumed 25% CO₂ relative abundance in the coma of comet C/2009 P1 in the model. Since CO is highly volatile and the comet is at a large heliocentric distance we assumed that the gas production rates for H₂O and CO are equal in this comet.

In comet C/2001 Q4 (NEAT), the H₂O production rate is measured by Biver et al. (2009) and Combi et al. (2009) at different heliocentric distances using hydrogen Ly- α (1216 Å) and radio (557 GHz) emissions, respectively. Combi et al. (2009)

fitted the observed H₂O production rate as a function of heliocentric distance (r_h) as $3.5 \times 10^{29} \times r_h^{-1.7}$ s⁻¹. We used this expression to calculate the H₂O production rate in this comet at 3.7 au where the green and red-doublet emissions were observed (Decock et al. 2013). Since the comet is at a large heliocentric distance we assumed that the CO and H₂O abundances are equal. Based on the observed G/R ratio on this comet, Decock et al. (2013) suggested that the CO₂ relative abundance in this comet could be between 60% and 80% with respect to H₂O. In our model we have assumed the CO₂ relative abundance at 3.7 au heliocentric distance to be 75%.

To evaluate the individual contributions of major O-bearing species in producing green and red-doublet emissions and their affect on the G/R ratio we have made a case study for a hypothetical comet X in which we assumed equal gas production of H₂O, CO₂, and CO in the comet. This is similar to the observation of Ootsubo et al. (2012) on comet C/2006 W3 in which it is found that CO₂ and H₂O gas production rates are equal ($\sim 8 \times 10^{27}$ s⁻¹); however, the CO production rate is around 3 times higher when the comet was at 3.7 au from the Sun.

The solar flux, which is required to calculate photorates of different species, is taken from the SOLAR2000 (S2K) v.2.36 model of Tobiska (2004) at 1 au and scaled according to the observed heliocentric distance of different comets. The electron temperature that determines the dissociative recombination rates of ions is taken as constant 300 K in the cometary coma. The effect of this constant temperature profile on the model calculation is discussed later. The yield of O(¹S) at solar H Ly- α in the photodissociation of H₂O is taken as 0.5%. The impact of this assumption was discussed in our previous work (Bhardwaj & Raghuram 2012). The photodissociative excitation cross section for CO₂ producing O(¹D) is taken from Jain (2013). The photorate for the production of O(¹S) from the photodissociation of CO has been taken from the theoretically estimated value of Festou & Feldman (1981) and scaled to the observed heliocentric distance.

3. Results

Since these comets have different water production rates (varying from 10²⁷ to 10²⁹ s⁻¹), as well as different CO₂ and CO relative abundances with respect to H₂O, we present calculations in comet C/2006 W3 which is followed by a discussion on the calculated results for other comets.

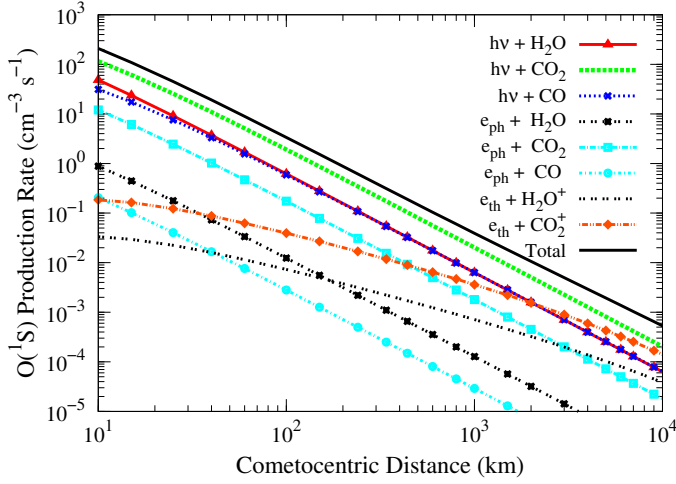


Fig. 1. Calculated volumetric $O(^1S)$ production rate profiles for major production mechanisms in comet C/2006 W3 (Christensen) with H_2O production rate of $2 \times 10^{28} \text{ s}^{-1}$ and 42% CO_2 and 98% CO abundances relative to H_2O in the cometary coma when the comet was at 3.13 au heliocentric distance. $h\nu$: solar photon; e_{ph} : photoelectron; and e_{th} : thermal electron.

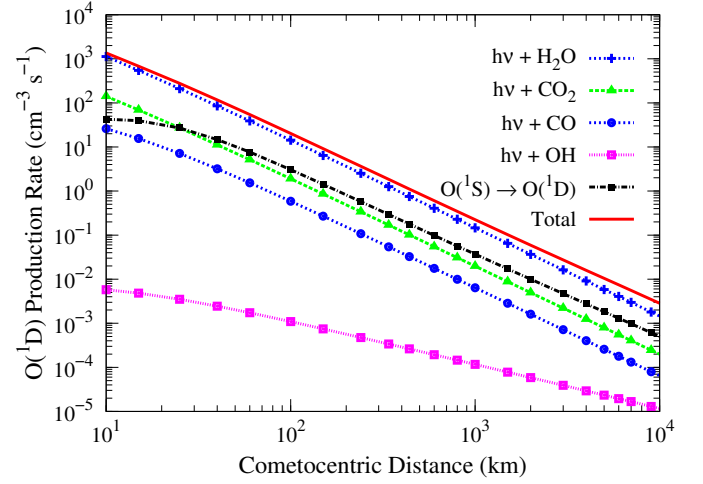


Fig. 2. Calculated volumetric $O(^1D)$ production rate profiles for major production mechanisms in comet C/2006 W3 (Christensen) with H_2O production rate of $2 \times 10^{28} \text{ s}^{-1}$ and 42% CO_2 and 98% CO relative abundances with respect to H_2O in the cometary coma when the comet was at 3.13 au from the Sun. $h\nu$: solar photon.

3.1. Production processes of $O(^1S)$ and $O(^1D)$

The calculated production rates for the $O(^1S)$ from different processes in comet C/2006 W3 are presented in Fig. 1. The major production source of oxygen atoms in the 1S metastable state is photodissociation of CO_2 followed by photodissociation of CO and H_2O . The contribution from the photoelectron impact excitation reactions is smaller compared to photodissociative excitation processes. Above 10^3 km, the dissociative recombination of CO_2^+ also contributes significantly. The solar flux in wavelength bin 955–1165 Å is the main source that dissociates CO_2 and produces atomic oxygen in the 1S state. Since the yield for photodissociation of CO_2 in this wavelength bin is almost unity, the absorption of solar photons of this wavelength bin by CO_2 leads to the formation of $O(^1S)$ and CO (Raghuram & Bhardwaj 2013; Bhardwaj & Raghuram 2012).

The calculated $O(^1D)$ production rate profiles for different mechanisms are shown in Fig. 2. The major production of $O(^1D)$ is via photodissociation of H_2O , but close to the nucleus (<30 km) photodissociation of CO_2 is also a significant $O(^1D)$ production process, and above 30 km the radiative decay of $O(^1S)$ becomes a more important source of $O(^1D)$ than the former. The photodissociation of CO and OH are minor production sources of $O(^1D)$. Most of the $O(^1D)$ production ($>95\%$) is due to photodissociation of H_2O by solar H Ly- α photon flux.

3.2. Loss processes of $O(^1S)$ and $O(^1D)$

The calculated $O(^1S)$ and $O(^1D)$ destruction rate profiles in comet C/2006 W3 are presented in Fig. 3. Since this comet has a low neutral gas production rate, the collisional quenching is a dominant $O(^1S)$ destructive mechanism only close to the nucleus (<30 km). The radiative decay which produces photons at 5577 Å and 2972 Å is the major loss process for $O(^1S)$ throughout the coma. The calculated loss rate profiles of $O(^1D)$ by various processes are also presented in the same figure. Below 300 km, quenching by H_2O and CO_2 are the dominant loss mechanisms of the $O(^1D)$. Above 300 km, the radiative decay, which results

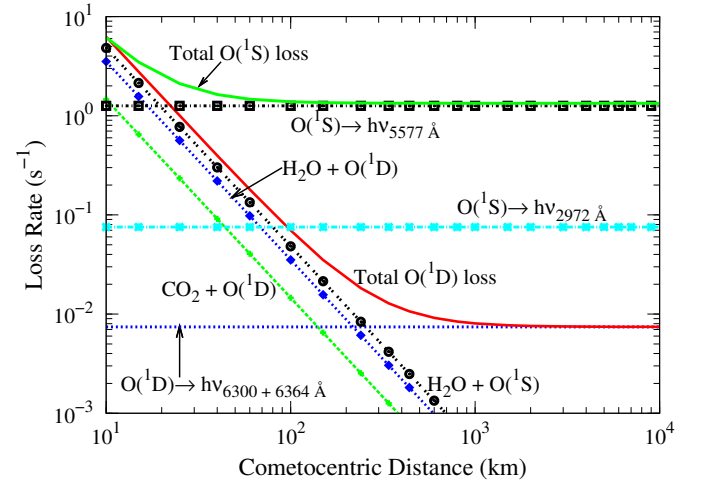


Fig. 3. Calculated radial loss rate profiles for major loss mechanisms of the $O(^1D)$ and $O(^1S)$ in comet C/2006 W3 (Christensen) with H_2O production rate of $2 \times 10^{28} \text{ s}^{-1}$ and 42% CO_2 and 98% CO abundances relative to H_2O in the cometary coma when the comet was at 3.13 au from the Sun.

in the emission of photons at 6300 Å and 6364 Å, is a major loss process for $O(^1D)$. Quenching by CO is a minor loss process for $O(^1D)$ which is not shown in the figure.

The calculated number density profiles of $O(^1S)$ and $O(^1D)$ in comet C/2006 W3 along with parent species H_2O , CO_2 , and CO are presented in Fig. 4. Close to the cometary nucleus the flatness in the calculated $O(^1S)$ and $O(^1D)$ number density profiles is due to collisional quenching by cometary species (mainly H_2O) and depends on the neutral gas production rate of the comet.

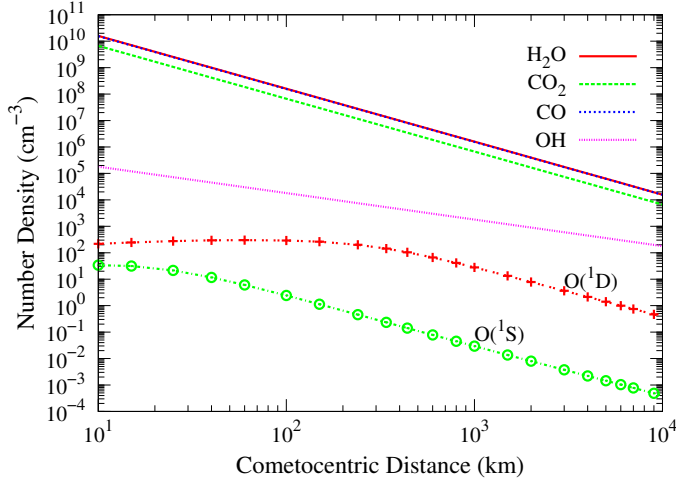


Fig. 4. Calculated number density profiles of $O(^1S)$, $O(^1D)$, and OH, along with those of H_2O , CO, and CO_2 in comet C/2006 W3 (Christensen) with H_2O production rate of $2 \times 10^{28} \text{ s}^{-1}$ and 42% CO_2 and 98% CO relative abundances with respect to H_2O in the cometary coma when the comet was at 3.13 au from the Sun.

3.3. [OI] green to red-doublet emission intensity ratio and line widths

The calculated number density profiles shown in Fig. 4 are multiplied with Einstein emission transition probabilities (see Table 1 in Raghuram & Bhardwaj 2013) to obtain emission rates. By integrating these emission rates along the line of sight we calculated the emission intensities of green and red-doublet lines as a function of projected distance. The calculated surface brightness profiles for [OI] 5577 Å and red-doublet (6300 + 6364 Å) emissions are shown in Fig. 5 with solid curves. It can be seen in this figure that close to the nucleus (below 40 km projected distance) the green line emission is more intense than the red-doublet emission, which is mainly due to the $O(^1S)$ emission rate (1.26 s^{-1}) being higher by about two orders of magnitude compared to that of $O(^1D)$ ($8.59 \times 10^{-3} \text{ s}^{-1}$). The calculated G/R ratio in comet C/2006 W3, which is shown with a dashed curve ("with CO") in Fig. 5, varies between 1.8 and ~0.2. In the same figure the calculated G/R ratio profiles for different cases are also presented. Since there is an uncertainty in the photo-rate of CO in producing $O(^1S)$, which is discussed later, we also did calculations for the G/R ratio neglecting this source mechanism which is shown in Fig. 5 with dotted curve ("without CO"). In this case the calculated G/R ratio varies between 1.6 and 0.18. Since comet C/2006 W3 has a very low gas production rate the collisional quenching may be less important. To assess the effect of collisional quenching on the green and red-doublet emissions, we calculated the G/R ratio without considering collisional destruction mechanisms of $O(^1S)$ and $O(^1D)$. In this case the calculated G/R ratio is a constant value of 0.18 throughout the coma which is represented with the dash-dotted line in Fig. 5.

Similarly, all these calculations have been carried out on other comets. Considering both collisional quenching and photodissociation of CO, the calculated G/R ratio profiles as a function of projected distance in six comets are presented in Fig. 6. This figure shows that close to the nucleus in comets C/2006 W3 and C/2001 Q4, the calculated G/R ratio value is more than one which is due to higher CO_2 relative abundances and strong collisional quenching of $O(^1D)$ by cometary species, whereas in other comets this value is always less than one throughout the coma.

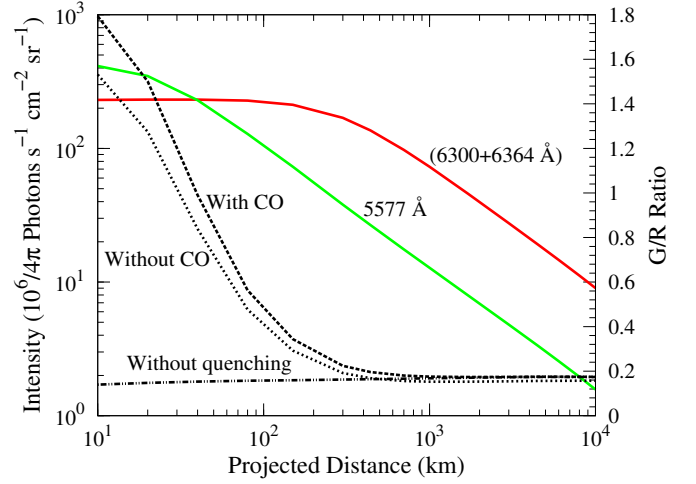


Fig. 5. Calculated [OI] red-doublet (6300+6364 Å) and 5577 Å line brightness profiles (with solid curves) along the cometocentric projected distances on comet C/2006 W3 (Christensen) with H_2O production rate of $2 \times 10^{28} \text{ s}^{-1}$ and 42% CO_2 and 98% CO relative abundances with respect to H_2O in the cometary coma when the comet was at 3.13 au from the Sun. The calculated G/R ratio profiles considering CO, without considering CO, and without quenching are plotted with dashed, dotted, and dash-dotted curves, respectively, on the right y-axis.

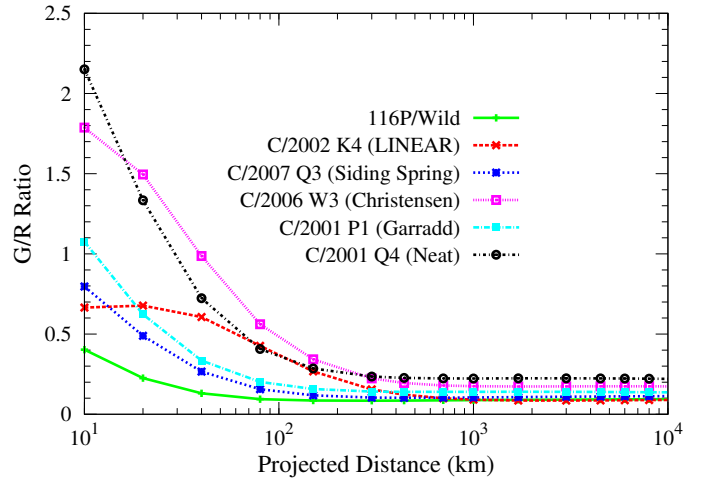


Fig. 6. The calculated radial profiles of the G/R ratio in different comets. The input parameters used to calculate the G/R ratio are tabulated in Table 1. It can be seen that in comets C/2006 W3 and C/2001 Q4, due to substantial collisional quenching of $O(^1S)$ and $O(^1D)$ with other cometary species, the calculated G/R ratio is more than 1 closer to the nucleus, whereas above 400 km projected distances it is a constant.

In comets C/2006 W3 and C/2001 Q4, the CO_2 abundances are very large (see Table 1) and no significant collisional quenching of $O(^1S)$. Thus, the green line intensity throughout the coma is determined by CO_2 and subsequently the G/R ratio governed by the quenching of $O(^1D)$ depending on the H_2O production rate. In other comets the G/R ratio is small because of lower CO_2 abundances compared to former comets.

We calculated the average G/R ratio over the observed projected area on each comet. The projected area on a comet changes with the dimension of slit used for observation and the geocentric distance of comet. The calculated averaged G/R ra-

tios on different comets are tabulated in Table 1 along with the values derived from observations. Our calculated G/R ratio values are comparable (within a factor of two) with the observations on different comets observed at different heliocentric and geocentric distances.

The percentage contributions for various production processes involved in the formation of $O(^1S)$ and $O(^1D)$ in these comets at three different projected distances are given in Table 2. These calculations suggest that in all these comets, the photodissociation of H_2O and CO_2 together produce 50–80% of $O(^1S)$, whereas, irrespective of CO_2 and CO relative abundances, the major (~50 to 80%) source for the formation of $O(^1D)$ is photodissociation of H_2O followed by radiative decay of $O(^1S)$ (10–15%). At larger projected distances ($>10^3$ km), dissociative recombination processes of H_2O^+ and CO_2^+ ions are also important production sources of $O(^1S)$ (30–40%) and $O(^1D)$ (~20%).

The calculated percentage contributions of different production processes in the total intensity of [OI] emissions over the observed coma on these comets are tabulated in Table 3. These calculations suggest that photodissociation of CO_2 and H_2O together contribute 50–70% to the green line emission and the remaining contribution is through dissociative recombination of H_2O^+ and CO_2^+ ions. In the case of red-doublet emission, photodissociation of H_2O and radiative decay of $O(^1S)$ together produce 70–90% and contributions from other sources are very small.

In the case of hypothetical comet X which has equal H_2O , CO_2 , and CO gas production rates, ~80% of green line emission intensity is governed by CO_2 (via photodissociation of CO_2 and dissociative recombination of CO_2^+), whereas photodissociation of H_2O and CO together contribute around 10%. Dissociative recombination of CO_2^+ is the second important source and contributes around 30% to the total green line emission. In this case around 35% of red-doublet emission is produced via H_2O photodissociation. The production of $O(^1D)$ via CO_2 photodissociation is around 10% of the total while it is ~25% via radiative decay of $O(^1S)$, which is also essentially produced from CO_2 . In this case both CO_2 and H_2O play equally important roles in producing red-doublet emission.

We also calculated the mean excess energy released in these photodissociative excitation reactions. The maximum excess energy in photodissociation of H_2O producing $O(^1S)$ by solar Ly- α photons is 1.27 eV, whereas the mean excess energy in the photodissociation of CO_2 forming $O(^1S)$ is 2.55 eV. Mean excess energies in photodissociative excitation of H_2O , CO_2 , and CO producing $O(^1D)$ are 1.12, 4.46, and 2.54 eV, respectively. We assumed that most of these excess energies will result in kinetic motion of daughter products. Thus, the excess velocities of $O(^1S)$ in photodissociative excitation of H_2O and CO_2 are 1.3 km s⁻¹ and 4.4 km s⁻¹, respectively. Similarly, the calculated excess velocities of $O(^1D)$ in photodissociation of H_2O , CO_2 , and CO are 1.6, 5.8, and 3.6 km s⁻¹, respectively.

Considering only photoreactions and using the calculated contributions of each process over the cometary coma (see Table 3) we calculated the mean excess energies of $O(^1S)$ and $O(^1D)$. Our calculated mean velocities of $O(^1S)$ and $O(^1D)$ atoms on these comets are tabulated in Table 3 along with the derived velocities based on the observed line widths. In comets having large CO_2 relative abundances the width of the green line, which is a function of mean $O(^1S)$ velocity, is mainly determined by photodissociation of CO_2 . Since the mean excess energy released in photodissociation of CO_2 is higher, the width of the green line would be greater compared to the red-doublet

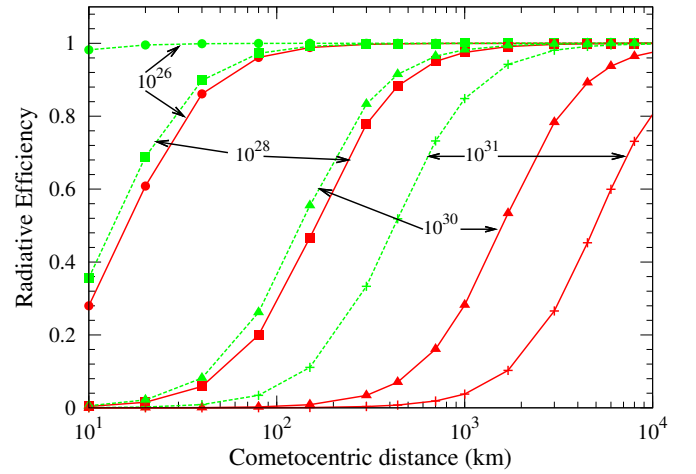


Fig. 7. The calculated radiative efficiency profiles of $O(^1S)$ (green lines) and $O(^1D)$ (red lines) for different production rates with 5% CO_2 and 10% CO relative abundances with respect to H_2O . The circles, squares, triangles, and cross symbols represent the calculated radiative efficiencies for the water production rates of 10^{26} , 10^{28} , 10^{30} , and 10^{31} , respectively.

emission line width (which is mainly determined by photodissociation of H_2O). Our calculated green line widths in different comets, which are presented in Table 3, are higher than the calculated red-doublet emission line widths, which is consistent with the observations.

Depending on the composition and activity of the nucleus, comets have different gas production rates at different heliocentric distances. In order to appraise the collisional quenching of $O(^1S)$ and $O(^1D)$ with increase in H_2O production rate, we calculated the radiative efficiencies of $O(^1S)$ and $O(^1D)$ for different water production rates. The calculated radiative efficiency profiles are shown in Fig. 7. This calculation shows that for a given water production rate the $O(^1D)$ is always much more quenched than that of $O(^1S)$. This is mainly because the lifetime of $O(^1D)$ (~120 s) is larger by two orders of magnitude than that of $O(^1S)$ (~0.8 s).

Since CO_2 is a potentially important source of $O(^1S)$ we have also carried out model calculations of the G/R ratio on different water production rates by varying its relative abundance from 0% to 100% with respect to H_2O . The calculations presented in Fig. 8 suggests that by increasing CO_2 relative abundance in a comet the G/R ratio increases almost monotonically.

4. Discussion

For comets close to 1 au from the Sun the dominant species in the cometary coma is H_2O . Because of lower ice-sublimation temperatures of CO and CO_2 , at large heliocentric distances the cometary coma is dominantly composed of CO_2 and CO (Meech & Svoreň 2004; Crovisier et al. 1999; Biver et al. 1997, 1999; Bockelée-Morvan et al. 2004, 2010). Owing to strong absorption of cometary H_2O infrared emission lines by terrestrial water molecules, it is difficult to detect H_2O in the coma for ground-based observations, but the spatial profiles of water can be easily derived in comets from ground-based observatories by

Table 2. Calculated percentage contributions for major production processes of O(¹S) and O(¹D) in different comets.

Comet	Production processes of O(¹ S) and O(¹ D) at three cometocentric projected distances (km) (%)																	
	hν + H ₂ O			hν + CO ₂			hν + CO			O(¹ S) → O(¹ D)			e _{th} ⁻ + H ₂ O ⁺			e _{th} ⁻ + CO ₂ ⁺		
	10 ²	10 ³	10 ⁴	10 ²	10 ³	10 ⁴	10 ²	10 ³	10 ⁴	10 ²	10 ³	10 ⁴	10 ²	10 ³	10 ⁴	10 ²	10 ³	10 ⁴
116P/Wild 4	43 (83)*	33 (71)	25 (59)	33 (3)	25 (2)	20 (2)	9 (0.5)	7 (0.5)	5 (0.5)				5 (4)	15 (14)	22 (22)	5 (0.1)	15 (0.7)	17 (2)
C/2003 K4 (LINEAR)	46 (88)	42 (83)	32 (71)	35 (3)	32 (3)	25 (2)	11 (1)	11 (1)	9 (1)	(7)	(8)	(9)	1 (0.5)	4 (3)	13 (13)	1 (0.5)	5 (0.5)	14 (1)
C/2007 Q3 (Siding Spring)	35 (82)	29 (73)	21 (60)	46 (4)	37 (4)	28 (3)	4 (0.5)	3 (0.5)	2 (0.5)	(9)	(10)	(11)	2 (2)	18 (9)	17 (20)	4 (0.5)	15 (2)	23 (3)
C/2006 W3 (Christensen)	18 (69)	15 (61)	11 (48)	55 (9)	47 (8)	37 (7)	17 (3)	15 (2)	11 (2)	(15)	(16)	(17)	0.5 (1)	3 (6)	8 (15)	3 (0.5)	15 (3)	28 (5)
C/2009 P1 (Garradd)	22 (71)	17 (58)	14 (47)	41 (6)	32 (5)	28 (4)	22 (3)	17 (3)	15 (2)	(13)	(14)	(13)	3 (4)	9 (14)	13 (19)	8 (1)	20 (3)	23 (3)
C/2001 Q4 (NEAT)	11 (57)	9 (47)	7 (37)	63 (13)	50 (11)	40 (9)	11 (2)	9 (2)	7 (2)	(21)	(22)	(22)	1 (2)	4 (8)	6 (14)	7 (1)	23 (5)	34 (8)
comet X**	8 (48)	6 (38)	5 (31)	63 (15)	47 (12)	41 (10)	8 (2)	6 (1)	5 (1)	(23)	(25)	(24)	1 (3)	3 (10)	5 (13)	12 (3)	30 (8)	37 (10)

*The values in parentheses are for O(¹D); **comet X is a hypothetical comet similar to the observational condition of comet NEAT and having equal gas production rates of H₂O, CO₂, and CO; hν = photon; e_{th}⁻ = thermal electron.

Table 3. Calculated percentage contributions for major production processes of green and red-doublet emissions in the slit projected field of view on different comets, and the comparison of the calculated and observed line widths.

Comet	hν + H ₂ O	hν + CO ₂	hν + CO	O(¹ S) → O(¹ D)	e _{th} ⁻ + H ₂ O ⁺	e _{th} ⁻ + CO ₂ ⁺	5577 Line width		6300 Line width	
							Cal***	Obs**	Cal***	Obs**
116P/Wild 4	34 (72)*	26 (2)	7 (0.5)	(9)	14 (13)	14 (1)	1.70	–	1.32	–
C/2003 K4 (LINEAR)	40 (81)	31 (3)	10 (1)	(8)	6 (5)	7 (0.5)	2.05	2.38–2.76	1.87	1.81–2.12
C/2007 Q3 (Siding Spring)	28 (72)	37 (4)	3 (0.5)	(10)	9 (10)	15 (1)	2.04	–	1.44	–
C/2006 W3 (Christensen)	14 (61)	47 (8)	14 (3)	(16)	3 (6)	15 (3)	2.48	–	1.58	–
C/2009 P1 (Garradd)	16 (55)	31 (4)	17 (3)	(13)	10 (15)	21 (3)	1.85	2.16–2.54	1.25	1.25–1.67
C/2001 Q4 (NEAT)	8 (44)	47 (11)	8 (2)	(22)	4 (9)	26 (6)	2.30	2.31–2.55	1.65	2.39–2.75
comet X****	6 (36)	46 (11)	6 (1)	(25)	4 (10)	31 (8)	2.35	–	1.65	–

*The values in parentheses are calculated percentage contributions for red-doublet emission; **Obs: observed line widths are taken from Decock et al. (2013); ***Cal: model calculated line widths; ****comet X is a hypothetical comet similar to the observational condition of comet NEAT and having equal gas production rates of H₂O, CO₂, and CO; hν = photon; e_{th}⁻ = thermal electron.

observing infrared H₂O non-resonance fluorescence emissions (Mumma et al. 1995, 1996; Dello Russo et al. 2000). Since H₂O does not have any transitions in the visible region the emissions of its daughter products have been used as tracers to understand the spatial distribution of water in the cometary coma. The observed atomic oxygen visible emissions (viz. O[¹I] 5577, 6300, and 6364 Å) have been used to quantify the H₂O production rate in several comets around 1 au (Delsemme & Combi 1976; Delsemme & Combi 1979; Fink & Johnson 1984; Schultz et al. 1992; Morgenthaler et al. 2001). Since CO₂ and CO can also produce these metastable oxygen atoms, based on the theoretical work of Festou & Feldman (1981), the G/R ratio of 0.1 has been used as the benchmark to confirm H₂O as the parent species for these oxygen emission lines. The available theoretical and experimental cross sections for the production of O(¹S) and O(¹D) from different O-bearing species have been reviewed in our previous work (Bhardwaj & Raghuram 2012).

Our coupled chemistry-emission model, which has been applied to comets Hyakutake and Hale-Bopp, suggested that the observed G/R ratio not only depends on the relative abundances of CO₂ and CO, but also on the projected area observed on the comet (Bhardwaj & Raghuram 2012).

Since CO₂ does not emit ultraviolet or visible photons we cannot detect this molecule directly in the cometary ultraviolet or visible spectra. Moreover, CO₂ is a symmetric molecule with no permanent dipole moment and so it is difficult to observe this molecule even in radio range from the ground (Ootsubo et al. 2012). Thus, this molecule is probed using indirect methods using the emissions of its dissociative products, like the CO Cameron band (a³Π–X¹Σ⁺) in ultraviolet (Weaver et al. 1994; Feldman et al. 1997) and visible atomic oxygen green and red-doublet emissions (Furusho et al. 2006; McKay et al. 2012; Decock et al. 2013). Our earlier works (Bhardwaj & Raghuram 2011; Raghuram & Bhardwaj

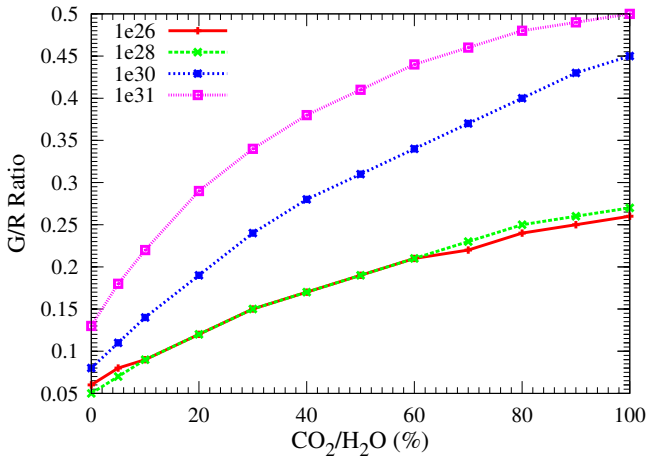


Fig. 8. The calculated G/R ratio as a function of CO₂ abundance for different water production rates, with 10% CO abundance relative to H₂O in the coma. These calculations are done at heliocentric and geocentric distances of 1 au using a square slit of side 5".

2012) have shown that CO Cameron band emission is not suitable for measuring CO₂ abundances in comets since this emission is mainly governed by photoelectron impact excitation of CO rather than the photodissociation of CO₂.

Assuming that the green line emission is governed by photodissociation of CO₂ while the red-doublet emission is controlled by photodissociation of H₂O, the observed G/R ratio has been used to quantify CO₂ relative abundance in the comets (McKay et al. 2012; Decock et al. 2013). At larger heliocentric distances CO₂ and CO are the dominant O-bearing species in the coma which can produce green and red-doublet emissions. In several comets the observed G/R ratio at large (>2 au) heliocentric distances is more than 0.1 (Decock et al. 2013; McKay et al. 2012; Furusho et al. 2006).

4.1. Impact of CO on the G/R ratio

At larger heliocentric distances, although CO abundance is substantial in the cometary comae, the photodissociation of CO is not a potential source of O(¹S) and O(¹D) atoms. This is mainly due to the proximity in the threshold energies of photodissociative excitation and photoionization of CO molecules. The threshold energies for dissociation of CO into O(¹D) and O(¹S) states are 14.35 and 16.58 eV, respectively, whereas it is 14 eV for ionization. Moreover, the branching ratio of ionization for the photons having energy more than 14 eV is ~0.98 (Huebner et al. 1992). Since the ionization energy is smaller than energy required in the formation of O(¹S) and O(¹D), most of the photons (>90%) having energy >14 eV ionize the CO molecule rather than causing photodissociative excitation. Based on Huebner & Carpenter (1979) compiled cross sections, Festou & Feldman (1981) estimated that the photodissociation of CO produces O(¹S) and O(¹D) with nearly equal rates. To evaluate the role of CO we also did calculations in comet C/2006 W3 by discarding photodissociation of CO as a source mechanism of both O(¹S) and O(¹D) (see Fig. 5). Though CO production rate is equal to that of H₂O in this comet (see Table 1), by removing CO contribution the calculated G/R ratio decreased by a maximum of about 10%. Similarly, our calculated percentage contribution over the observed coma on different comets, which is presented in Table 3, also suggests that the

role of CO is very small (<20%) in producing O(¹S) and O(¹D) atoms and subsequently in determining the red-doublet emission intensity. Even without considering photodissociation of CO in the model the calculated G/R ratio values are in agreement with the observations. Based on these calculations we can suggest that the photodissociation of CO is an insignificant source of O(¹S) and O(¹D). Hence, the photodissociation of CO has almost no impact on the G/R ratio.

4.2. Impact of CO₂ on the G/R ratio

The relative abundance of CO₂ with respect to H₂O, is very important in determining the G/R ratio. This can be understood from the calculated G/R ratio profiles on comets 116P, C/2007 Q3, and C/2001 Q4, which have nearly same H₂O production rates ($1-4 \times 10^{28} \text{ s}^{-1}$), but different relative abundances of CO₂ and CO, and are observed at different heliocentric distances (see Fig. 6). As discussed in Section 4.1, the CO abundance does not have any appreciable impact on the G/R ratio. Hence, the change in the calculated G/R ratio on these comets can be ascribed mainly to the difference in CO₂ relative abundances. The calculated G/R ratio profiles on these comets are shown in Fig. 6, which shows that by increasing CO₂ the G/R ratio increases. In comet C/2001 Q4, due to higher (75%) CO₂ relative abundance, the calculated G/R ratio value is more than one close to the cometary nucleus. Similar behaviour is seen for comet C/2006 W3 which is due to larger (~40%) CO₂ relative abundance with respect to H₂O, and also due to significant collisional quenching of O(¹D) (see Fig. 5). We found that by doubling CO₂ relative abundance the G/R ratio changes by ~25%, whereas collisional quenching alone can vary its value by an order of magnitude. The model calculated G/R ratio values in comets 116P, C/2007 Q3, and C/2009 P1 are smaller by a factor of around 1.5 compared to the observations.

The detection of CO₂ molecules in the coma has been carried out using several infrared satellites by observing its fundamental vibrational band emission (ν_3) at 4.26 μm (Crovisier et al. 1996, 1997, 1999; Colangeli et al. 1999; Reach et al. 2010; Ootsubo et al. 2012). The quantification of CO₂ abundance based on the observed infrared emission intensity is subjected to opacity of the cometary coma. Since the CO₂ fluorescence efficiency factor (g -factor) is larger compared to that of H₂O and CO (see Table 2 of Ootsubo et al. 2012), these emission lines are optically thick in the inner coma, which can result in underestimation of CO₂ abundance if proper treatment of radiative transfer is not accounted for in the analysis. The optical depth effects in the inner coma may cause the surface brightness profile of these emissions to be much flatter and resemble the presence of extended sources in the coma. In comet Hale-Bopp, Bockelée-Morvan et al. (2010) have shown that the observed broad extent of infrared CO brightness is due to optical depth effects of the emitted radiation and not because of extended sources. Since these comets are observed at larger heliocentric distances and have low gas production rates, the collision dominated coma size is only a few hundred kilometers. Thus, the opacity effects of these IR emissions can be significant close to the nucleus and can influence the derivation of CO₂ production rate based on the observed flux over the field of view. The discrepancies between the Ootsubo et al. (2012) derived production rates and other observations might be due to opacity of the cometary comae or may be due to assumed input parameters in the derivation of gas production rates. Under assumed optically thin condition the Ootsubo et al. (2012) derived gas production rates in several comets can be regarded as lower limits. Con-

sidering these observational facts we varied CO₂ abundances in the model to assess our model calculated G/R ratio with the observations. By increasing CO₂ abundances in these comets by a factor of 3 we could achieve better agreement with the observed G/R ratio.

Similarly, the calculations presented in Fig. 8 demonstrate that for a constant H₂O production rate, the G/R ratio increases with increasing CO₂ relative abundance. This figure suggests that for a constant CO₂ relative abundance, by increasing the H₂O production rate, the collisional quenching of O(¹S) and O(¹D) can increase the G/R ratio. Thus, the observation of a larger G/R ratio value need not be always due to higher CO₂ abundances.

In the case of hypothetical comet X, which has CO₂ abundance equal to that of H₂O, the calculated percentage contributions of different processes to red-doublet emissions presented in Table 3 suggest that the red-doublet emission intensity is equally controlled by CO₂ and H₂O. If a comet has equal abundances of CO₂ and H₂O, which is the case for comet C/2006 W3 observed by Ootsubo et al. (2012) at 3.7 au from the Sun, deriving the water production rates based on the observed red-doublet emission intensity may result in over estimation of H₂O. In this case the derivation of CO₂ abundances using the observed G/R ratio also leads to improper estimation. This calculation suggests that in a comet having high CO₂ abundance, the red-doublet emission intensity is not suitable for measuring H₂O rates. Similarly, our model calculations on comet C/2001 Q4, which has 75% CO₂ relative abundance, suggest that around 30% of red-doublet emissions are governed by both photodissociation of CO₂ and radiative decay of O(¹S), which is comparable to the contribution from H₂O (~45%) (see Table 3).

4.3. Impact of collisional quenching of O(¹S) and O(¹D) on the G/R ratio

The G/R ratio at a given projected distance mainly depends on the formation and destruction processes of excited oxygen atoms in the cometary coma along the line of sight. The abundances of O-bearing species and solar flux governs the formation rate of these metastable species while the chemical lifetime and collisional quenching by other cometary species determines the destruction rate. In a comet having moderate H₂O production rate of $4 \times 10^{28} \text{ s}^{-1}$, the radius of the H₂O collisional zone is around 1000 km (Whipple & Huebner 1976). When the comet is at a larger heliocentric distance, a lower gas evaporation rate results in a smaller collisional coma. Discarding the collisional quenching effect the observed G/R ratio has been used to infer CO₂ production rate in comets observed at large heliocentric distances (McKay et al. 2012; Decock et al. 2013). Our calculated G/R ratio values as a function of projected distance on different comets (cf. Figures 5 and 6) have shown that the collisional quenching of O(¹S) and O(¹D) can result in larger (even > 1) G/R ratio values. Since the G/R ratio is averaged over the observed large projected distances, the collisional quenching may not influence the average value. In this case the observed G/R ratio is mainly determined by photochemical reactions of H₂O and CO₂ in producing red and green emissions, respectively. Hence, the observed G/R ratio value can be used to estimate the upper limit of CO₂ abundance relative to the H₂O production rate. But in the case of observations over smaller projected distances the collisional zone can predominantly affect the observed G/R ratio value which eventually can lead to the estimation of higher CO₂ abundances. Since the comets considered in this study are observed over large projected distances the effect of collisional

quenching is small on the averaged G/R ratio. In such cases the observed G/R ratio value can be effective in constraining the upper limit of the CO₂ relative abundance.

4.4. Green and red-doublet emission line widths

Cochran (2008) made high-resolution observations on different comets and found that the green line width is higher than both red-doublet emission lines. The observation of these forbidden lines made on 12 comets have also shown the same feature (Decock et al. 2013). The wider green line implies higher mean velocity distribution of O(¹S) atoms in the cometary coma. The high velocity of O(¹S) atoms in the cometary coma could be due to a parent source other than H₂O or could be due to involvement of high energy photons in H₂O dissociation. Our model calculations on comet Hale-Bopp showed that CO₂ photodissociation is a potentially more important source than that of H₂O in producing O(¹S) atoms with high excess velocity (Raghuram & Bhardwaj 2013).

From the calculations presented in Table 3, it can be understood that both CO₂ and H₂O are the important sources of O(¹S), whereas O(¹D) is mainly sourced from H₂O. Since high energy photons (955–1165 Å) mainly dissociate CO₂ and produce O(¹S), the mean excess energy released in this reaction is larger (~2.5 eV) compared to that of H₂O (~1.2 eV). This results in the production of O(¹S) atoms with large velocities (4.3 km s⁻¹) in cometary coma. The calculations presented in Table 3 show that above 10⁴ km projected distances, the thermal recombination of H₂O⁺ and CO₂⁺ ions together results in the production of 15–40% of O(¹S) and around 20% of O(¹D). Rosén et al. (2000) and Seiersen et al. (2003) experimentally determined the excess energies and branching ratios for the dissociative products in dissociative recombination of H₂O⁺ and CO₂⁺ ions, respectively. Based on these measured branching fractions and by theoretical estimation, we calculated the excess velocities of O(¹S) and O(¹D) and green and red line widths by incorporating the dissociative recombination reactions. We found an increase in our calculated green and red line widths by a factor of 1.2–1.7 and 1.1–2.2, respectively. However, without accounting for dissociative recombination reactions in our model, the calculated G/R ratio values (see Table 1) and line widths (see Table 3) are consistent with the observations. In comet C/2001 Q4 our calculated red line width is smaller than the observed value. It can be noticed that in this comet both green and red-doublet line widths are nearly the same and the red line widths are higher compared to those on other comets, which is difficult to explain based on the model calculations.

Our calculations show that the dissociative recombination of H₂O⁺ and CO₂⁺ ions are an important source of O(¹S) in the outer coma. In the model calculations we assumed a constant electron recombination temperature of 300 K. Since comets are observed at large heliocentric distances the temperature values can be less than 300 K. To study the effect of electron temperature on the calculated G/R ratio and line widths we decreased the temperature to 200 K. We did not find any noticeable change in the calculated G/R ratio values or line widths. Since most of the green and red-doublet emission intensities are determined by photodissociation reactions in the inner coma the contribution of thermal recombination of ions on the averaged G/R ratio is rather small.

Several observations beyond 2 au have shown that the H₂O production rate in comets does not vary as a function of the inverse square of heliocentric distance (Biver et al. 1997, 1999,

2007; Bodewits et al. 2012). Hence, extrapolation of the H_2O production rate based on an approximation of the inverse square of heliocentric distance may be inappropriate. We evaluated the implications of this extrapolation in comet C/2003 K4 by decreasing the H_2O production rate by a factor of 2. No significant change (decrease by $\leq 5\%$) is observed in the model calculated G/R ratio and the calculated line widths.

4.5. Effect of atmospheric seeing

For small ($0.6\text{--}2''$) slit observations the differential atmospheric seeing can be an issue while determining the G/R ratio based on the observed atomic oxygen green and red-doublet line emission fluxes. The work carried out by McKay et al. (2014) suggests that the differential refraction is potentially important for the near UV (e.g. CN 3870 Å) compared to the observation in the wavelength region 5000–6500 Å. They calculated the effect of differential refraction to be around 5% or less. In order to estimate the atmospheric seeing effect in determining slit-averaged G/R ratio we convolved our model calculated green and red-doublet emission fluxes with Gaussian function with full width at half maximum of seeing value $1.0''$. All these comets, except 116P, considered in the present work have been observed at larger (>2 au) geocentric distances; hence, the projected area on these comets would be larger.

In comet C/2001 Q4, which was observed at $r = 3.7$ au and $\Delta = 3.4$ au, the model calculated G/R ratio varies between 2.2 and 0.2 below 100 km projected distance (cf. Figures 6 and 9). After incorporating the seeing effect we found that the calculated G/R ratio is a constant throughout the projected distances with a value of about 0.2 as shown in Fig. 9. However, we do not find any change in the slit-averaged G/R ratio after accounting for the seeing effect in the model. Since the slit-averaged G/R ratio is over a much larger projected area, while the seeing effect is confined to distances close to the nucleus (cf. Fig. 6). We also assessed the output by changing the seeing value (from $1.0''$ to $0.5''$). No appreciable change in the modelled G/R ratio is observed. This suggests that the atmospheric seeing effect does not influence the G/R ratio for the comets observed at larger (>2 au) geocentric distances. Detailed analysis of the atmospheric seeing on different comets observed at different geocentric distances (< 2 au) are being carried out and will be presented in our next paper (Decock et al. 2014, in preparation).

5. Summary and conclusion

The observation of green and red-doublet emission lines in comets at larger (> 2 au) heliocentric distances suggest that the G/R ratio value is larger than 0.1. Moreover, the high-resolution observation reports that the green line is wider than the red-doublet lines, which is difficult to explain based on the single parent source for these oxygen emission lines (Decock et al. 2013). We have developed a coupled chemistry-emission model for atomic oxygen visible prompt emissions and applied it on six comets, (viz. 116P/Wild 4, C/2003 K4 (LINEAR), C/2007 Q3 (Siding Spring), C/2006 W3 (Christensen), C/2009 P1 (Garradd), C/2001 Q4 (NEAT)) which are observed at heliocentric distances greater than 2 au. By accounting for important chemical reactions in the model we calculated the G/R ratio values and widths of green and red-doublet emission lines on these comets. It is found that CO_2 is potentially more important than H_2O in

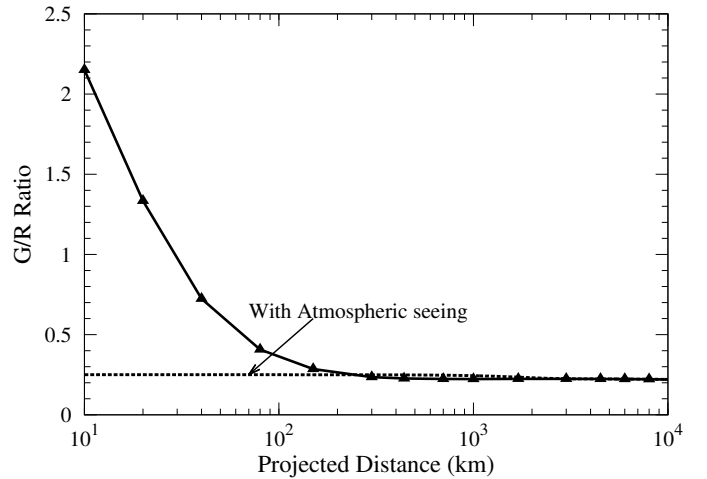


Fig. 9. The model calculated G/R ratio on comet C/2001 Q4 (NEAT) at $r = 3.7$ au and $\Delta = 3.4$ au. The black dashed line is the calculated G/R ratio after convolving with a Gaussian function of full width at half maximum of $1.0''$ seeing value.

$\text{O}(^1\text{S})$ production while $\text{O}(^1\text{D})$ is mainly controlled by H_2O . The photodissociation of CO is an insignificant source of metastable oxygen atoms. The observed large green line width in several comets is due to higher velocity of $\text{O}(^1\text{S})$ atoms that are essentially produced via photodissociation of CO_2 by higher energy (955–1165 Å) photons. We have shown that the collisional quenching of $\text{O}(^1\text{S})$ and $\text{O}(^1\text{D})$ by H_2O can lead to a larger G/R ratio value and that its impact on the G/R ratio is larger than the change in CO_2 relative abundance. Hence, the larger G/R ratio value need not always be linked to larger CO_2 abundances. In a comet having large ($>50\%$) CO_2 abundances, the photodissociation of CO_2 plays a significant role in producing both green and red-doublet emissions; thus, this process should also be accounted for while deriving the H_2O production rate based on the red-doublet emission intensity. When a comet is observed over a larger projected distance where the collisional zone is less resolvable, the collisional quenching does not affect the observed G/R ratio. At larger heliocentric distances, due to smaller gas production rates, the radius of a collisional coma is smaller; hence, the G/R ratio observed over larger projected distances can be used to constrain the CO_2 relative abundance. However, if the slit-projected area on the comet is smaller (with respect to the collisional zone), the derived CO_2 abundance based on the G/R ratio would be overestimated. Our model calculated G/R ratio and line widths of green and red-doublet emission are in agreement with the observation.

Acknowledgements. S. Raghuram was supported by the ISRO Senior Research Fellowship during the period of this work. Solar Irradiance Platform historical irradiances are provided courtesy of W. Kent Tobiska and Space Environment Technologies. These historical irradiances have been developed with partial funding from the NASA UARS, TIMED, and SOHO missions. We thank Alice Decock, Jeffrey P. Morgenthaler, and Adam McKay for the helpful discussions on the seeing effect on observation of comets.

References

- Bhardwaj, A. 1999, *J. Geophys. Res.*, 104, 1929
- Bhardwaj, A. & Haider, S. A. 2002, *Adv. Space Res.*, 29, 745
- Bhardwaj, A. & Raghuram, S. 2011, *Mon. Not. R. Astron. Soc.*, 412, L25
- Bhardwaj, A. & Raghuram, S. 2012, *Astrophys. J.*, 748, 13
- Biver, N., Bockelée-Morvan, D., Colom, P., et al. 1997, *Science*, 275, 1915
- Biver, N., Bockelée-Morvan, D., Colom, P., et al. 2009, *Astron. Astrophys.*, 501, 359

- Biver, N., Bockelée-Morvan, D., Crovisier, J., et al. 1999, *Astron. J.*, 118, 1850
- Biver, N., Bockelée-Morvan, D., Crovisier, J., et al. 2007, *Planetary and Space Science*, 55, 1058
- Bockelée-Morvan, D., Crovisier, J., Mumma, M. J., & Weaver, H. A. 2004, *The composition of cometary volatiles: Comets II*, ed. Festou, M. C., Keller, H. U., & Weaver, H. A., 391–423
- Bockelée-Morvan, D., Hartogh, P., Crovisier, J., et al. 2010, *Astron. Astrophys.*, 518
- Bodewits, D., Farnham, T. L., & A'Hearn, M. F. 2012, in *AAS/Division for Planetary Sciences Meeting Abstracts*, Vol. 44, AAS/Division for Planetary Sciences Meeting Abstracts, 506.06
- Capria, M. T., Cremonese, G., Bhardwaj, A., & de Sanctis, M. C. 2005, *Astron. Astrophys.*, 442, 1121
- Capria, M. T., Cremonese, G., Bhardwaj, A., Sanctis, M. C. D., & Epifani, E. M. 2008, *Astron. Astrophys.*, 479, 257
- Capria, M. T., Cremonese, G., & de Sanctis, M. C. 2010, *Astron. Astrophys.*, 522, A82
- Cochran, A. L. 2008, *Icarus*, 198, 181
- Cochran, A. L. & Cochran, W. D. 2001, *Icarus*, 154, 381
- Cochran, W. D. 1984, *Icarus*, 58, 440
- Colangeli, L., Epifani, E., Brucato, J. R., et al. 1999, *Astron. Astrophys.*, 343
- Combi, M. R., Mäkinen, J. T. T., Bertaux, J. L., Lee, Y., & Quémerais, E. 2009, *Astron. J.*, 137, 4734
- Combi, M. R., Mäkinen, J. T. T., Bertaux, J.-L., et al. 2013, *Icarus*, 225, 740
- Crovisier, J., Brooke, T. Y., Hanner, M. S., et al. 1996, *Astron. Astrophys.*, 315, L385
- Crovisier, J., Leech, K., Bockelée-Morvan, D., et al. 1997, *Science*, 275, 1904
- Crovisier, J. T. E., Lellouch, E., Bockelée-Morvan, D., et al. 1999, *Proceedings of the conference "The Universe as seen by ISO"*, 121, 161
- Decock, A., Jehin, E., Hutsemékers, D., & Manfroid, J. 2013, *Astron. Astrophys.*, 555, A34
- Dello Russo, N., Mumma, M. J., Disanti, M. A., et al. 2000, *Icarus*, 143, 324
- Delsemme, A. H. & Combi, M. R. 1976, *Astrophys. J. Lett.*, 209, L149
- Delsemme, A. H. & Combi, M. R. 1979, *Astrophys. J.*, 228, 330
- Farnham, T. L., Bodewits, D., A'Hearn, M. F., & Feaga, L. M. 2012, in *AAS/Division for Planetary Sciences Meeting Abstracts*, Vol. 44, AAS/Division for Planetary Sciences Meeting Abstracts, 506.5
- Feaga, L. M., A'Hearn, M., Farnham, T., et al. 2012, in *AAS/Division for Planetary Sciences Meeting Abstracts*, Vol. 44, AAS/Division for Planetary Sciences Meeting Abstracts, 313.08
- Feldman, P. D., Festou, M. C., Tozzi, G. P., Feldman, P. D., & Weaver, H. A. 1997, *Astrophys. J.*, 475, 829
- Festou, M. C. & Feldman, P. D. 1981, *Astron. Astrophys.*, 103, 154
- Fink, U. & Johnson, J. R. 1984, *Astron. J.*, 89, 1565
- Furusho, R., Kawakita, H., Fuse, T., & Watanabe, J. 2006, *Adv. Space Res.*, 9, 1983
- Haider, S. A. & Bhardwaj, A. 2005, *Icarus*, 177, 196
- Huebner, W. F. & Carpenter, C. W. 1979, *Los Alamos Report*, 8085
- Huebner, W. F., Keady, J. J., & Lyon, S. P. 1992, *Astrophys. Space Sci.*, 195, 1
- Huestis, D. L. & Slanger, T. G. 2006, *American Astronomical Society*, 38, 62.20
- Jain, S. K. 2013, *Phd. Thesis: Dayglow emissions on Mars and Venus*
- McKay, A. J., Chanover, N. J., Morgenthaler, J. P., et al. 2012, *Icarus*, 277
- McKay, A. J., Chanover, N. J., Disanti, M. A., Morgenthaler, et al. 2014, *Icarus*, 193
- Meech, K. J. & Svoreň, J. 2004, *Using Cometary Activity to Trace the Physical and Chemical Evolution of Cometary Nuclei* (M. C. Festou, H. A. Weaver, & H. U. Keller (Ed.)(Tucson: Univ. of Arizona)), 317–335
- Morgenthaler, J. P., Harris, W. M., Scherb, F., et al. 2001, *Astrophys. J.*, 563, 451
- Morrison, N. D., Knauth, D. C., Mulliss, C. L., & Lee, W. 1997, *Astro. Soc. Pac.*, 109, 676
- Mumma, M. J., DiSanti, M. A., Dello Russo, N., et al. 1996, *Science*, 272, 1310
- Mumma, M. J., DiSanti, M. A., Tokunaga, A., & Roettger, E. E. 1995, *Bull. Am. Astron. Soc.*, 27, 1144
- Ootsubo, T., Kawakita, H., Hamada, S., et al. 2012, *Astrophys. J.*, 752, 1
- Paganini, L., Mumma, M. J., Villanueva, G. L., et al. 2012, *Astrophys. J. Lett.*, 748
- Raghuram, S. & Bhardwaj, A. 2012, *Planetary and Space Science*, 63–64, 139
- Raghuram, S. & Bhardwaj, A. 2013, *Icarus*, 223, 91
- Reach, W. T., Vaubailon, J., Lisse, C. M., Holloway, M., & Rho, J. 2010, *Icarus*, 208, 276
- Rosén, S., Derkatch, A., Semaniak, J., et al. 2000, *Faraday Discuss.*, 407, 295
- Schultz, D., Li, G. S. H., Scherb, F., & Roesler, F. L. 1992, *Icarus*, 96, 190
- Seiersen, K., Al-Khalili, A., Heber, O., et al. 2003, *Phys. Rev. A*, 68
- Tobiska, W. K. 2004, *Adv. Space Res.*, 34, 1736
- Villanueva, G. L., Mumma, M. J., DiSanti, M. A., et al. 2012, *Icarus*, 220, 291
- Weaver, H. A., Feldman, P. D., McPhate, J. B., et al. 1994, *Astrophys. J.*, 422, 374
- Whipple, F. L. & Huebner, W. F. 1976, *Ann. rev. Astron. Astrophys.*, 14, 143
- Woodward, C. E., Kelley, M. S., Bockelée-Morvan, D., & Gehrz, R. D. 2007, *Astrophys.*, 671, 1065
- Zhang, H. W., Zhao, G., & Hu, J. Y. 2001, *Astron. Astrophys.*, 367, 1049